Supporting Information for

# Bimetallic Metal–organic Framework Catalyst *via* Selective Detection & Adsorption of $Fe^{3+}$ for Enhanced Bio-based Catalysis

Man Wang,[a] Fangmin Huang,[a] Chan Wang,[b] Yuanyuan Hu,[a] Pengyan Wu,*[a] Aonan Hu,[a] Jingwen Ji[a] and Jian Wang*[a]

[a] School of Chemistry and Materials Science & Jiangsu Key Laboratory of Green Synthetic Chemistry for Functional Materials, Jiangsu Normal University, Xuzhou, Jiangsu, 221116, People's Republic of China.

[b] Yantai Centre for Promotion of Science and Technology Innovation, Yantai, Shandong 264003, P.R. China

**Materials and Methods**.

**Reagents and chemicals:** All reagents and solvents were of AR grade and used without further purification unless otherwise noted. 2,2',3,3'-oxydiphthalic acid was purchased from Jinan Henghua Sci. & Tec. Co., Ltd., fructose, glucose and $Tb(NO_3)_3·6H_2O$ were purchased from Alfa Aesar, $Fe(NO_3)_3·9H_2O$ and the other metal salts were provided from Shanghai Fourth Chemical Reagent Company (China). Stock solution ($2×10^{-2}$ M) of the aqueous nitrate salts of $Li^+$, $Na^+$, $K^+$, $Mg^{2+}$, $Ca^{2+}$, $Sr^{2+}$, $Ba^{2+}$, $Co^{2+}$, $Ni^{2+}$, $Cu^{2+}$, $Mn^{2+}$, $Zn^{2+}$, $Cd^{2+}$, $Fe^{2+}$, $Ag^+$, $Pb^{2+}$, $Al^{3+}$, $Cr^{3+}$, $Fe^{3+}$ and $Hg^{2+}$ were prepared for further experiments.

**Instruments and spectroscopic measurements:** X-ray powder diffraction (XRD) patterns of the Tb−HODA was recorded on a Rigaku D/max-2400 X-ray powder diffractometer (Japan) using Cu-Kα ($\lambda$ =1.5405 Å) radiation. Elemental analyses (C, H, O) were performed on an Elementar Vario EL analyzer. The metal content were measured by Inductively Coupled Plasma Spectrometer (Perkin Elmer). X-ray photoelectron spectroscopy (XPS) experiments were performed with a PHI QUANTUM2000 surface analysis instrument. The morphologies of the prepared samples were recorded by a Field Emission Scanning Electron Microscopy (SEM) of Hitachi SU8010. Samples were treated *via* Pt sputtering for 90 s before observation. And energy dispersive X-ray spectroscopy (EDS) images were captured with an equipment of EDAX PW9900. FT−IR spectra were recorded as KBr pellets on JASCO FT/IR−430. Pyridine Fourier-transform infrared (Py-FTIR) spectroscopy was performed using a USA PE Frontier FT-IR spectrometer. The sample was inserted into a measurement cell with KBr windows that was connected to a vacuum. The sample was treated at 350 °C under vacuum for 2 h and was subsequently cooled to room temperature to collect the background spectra. Pyridine adsorption was performed by equilibrating the sample for 30 min at room temperature. To calculate the weak acidic sites and strong acidic sites, the IR spectra for the samples were recorded after degassing for 60 min at 150 °C. Fluorescence spectra of the solution were obtained using the F−4600 spectrometer (Hitachi), and the relative fluorescence intensity is used to normalize the fluorescence intensity to eliminate the influence of initial fluorescence on the measurement. Both excitation and emission slit widths were 2.5 nm. Fluorescence measurements were carried out in a 1 cm quartz cuvette with stirring the suspension of Tb−HODA. HMF concentration was determined using high-performance liquid chromatography (HPLC, Agilent 1200) using a column (Zorbax SB-C18) with a UV detector to analyze HMF yield.

**X-ray Crystallography (Single-crystal diffraction) and Characterizations**.

**Crystal data of Tb−HODA:**

$C_{16}H_7O_{14}Tb$, Mr = 582.14, Monoclinic, space group $P2(1)/n$, $a$ = 13.779(3), $b$ = 10.880(2), $c$ = 14.024(3) Å, $\alpha$ = 90.00, $\beta$ = 116.737(5), $\gamma$ = 90.00, $V$ = 1877.6(7) Å$^3$, $Z$ = 4, $D$c = 2.059g cm$^{-3}$, $\mu$(Mo-Kα) = 3.844 mm$^{-1}$, $T$ = 153(2) K. 10397 unique reflections [$R_{\text{int}}$ = 0.0444]. Final $R_1$[with $I > 2\sigma(I)$] = 0.0405, $wR_2$(all data) = 0.1115, GOOF = 1.014. CCDC number: 2048206.

**Crystallography**:

Intensities were collected on a Bruker SMART APEX CCD diffractometer with graphite monochromated Mo-$K\alpha$ ($\lambda$ = 0.71073 Å) using the SMART and SAINT programs. The structure was solved by direct methods and refined on $F^2$ by full-matrix least-squares methods with SHELXTL *version* 5.1. Non-hydrogen atoms of the ligand backbones were refined anisotropically. Hydrogen atoms within the ligand backbones were fixed geometrically at calculated positions and allowed to ride on the parent non-hydrogen atoms. Hydrogen atoms of the carboxylate moieties were found from the difference Fourier maps and refined with the isotropic parameters fixed as 1.5 times of those oxygen atoms they attached and with the O−H distance fixed at 0.85Å.

**Table S1.** Selective bond distance (Å) and angle (°) in **Tb−HODA**.

| | | | |
|---|---|---|---|
| Tb(1)–O(7) | 2.311(5) | Tb(1)–O(2W) | 2.386(5) |
| Tb(1)–O(3W) | 2.397(6) | Tb(1)–O(8A) | 2.408(6) |
| Tb(1)–O(1W) | 2.451(6) | Tb(1)–O(4) | 2.453(5) |
| Tb(1)–O(3) | 2.457(5) | Tb(1)–O(9A) | 2.483(5) |

| | | | |
|---|---|---|---|
| Tb(1)–O(4W) | 2.601(11) | | |
| O(7)–Tb(1)–O(2W) | 76.28(18) | O(7)–Tb(1)–O(3W) | 88.2(2) |
| O(2W)–Tb(1)–O(3W) | 144.0(2) | O(7)–Tb(1)–O(8A) | 148.3(2) |
| O(2W)–Tb(1)–O(8A) | 92.5(2) | O(3W)–Tb(1)–O(8A) | 83.8(2) |
| O(7)–Tb(1)–O(1W) | 77.3(2) | O(2W)–Tb(1)–O(1W) | 74.6(2) |
| O(3W)–Tb(1)–O(1W) | 70.3(2) | O(8A)–Tb(1)–O(1W) | 71.1(2) |
| O(7)–Tb(1)–O(4) | 79.78(17) | O(2W)–Tb(1)–O(4) | 83.85(18) |
| O(3W)–Tb(1)–O(4) | 125.57(18) | O(8A)–Tb(1)–O(4) | 129.16(19) |
| O(1W)–Tb(1)–O(4) | 151.6(2) | O(7)–Tb(1)–O(3) | 77.58(18) |
| O(2W)–Tb(1)–O(3) | 132.69(17) | O(3W)–Tb(1)–O(3) | 72.57(19) |
| O(8A)–Tb(1)–O(3) | 128.1(2) | O(1W)–Tb(1)–O(3) | 135.3(2) |
| O(4)–Tb(1)–O(3) | 53.02(15) | O(7)–Tb(1)–O(9A) | 145.67(17) |
| O(2W)–Tb(1)–O(9A) | 76.2(2) | O(3W)–Tb(1)–O(9A) | 126.0(2) |
| O(8A)–Tb(1)–O(9A) | 52.94(18) | O(1W)–Tb(1)–O(9A) | 114.2(2) |
| O(4)–Tb(1)–O(9A) | 77.24(17) | O(3)–Tb(1)–O(9A) | 107.4(2) |
| O(7)–Tb(1)–O(4W) | 137.6(3) | O(2W)–Tb(1)–O(4W) | 141.9(3) |
| O(3W)–Tb(1)–O(4W) | 67.9(3) | O(8A)–Tb(1)–O(4W) | 66.1(4) |
| O(1W)–Tb(1)–O(4W) | 122.0(4) | O(4)–Tb(1)–O(4W) | 86.4(3) |
| O(3)–Tb(1)–O(4W) | 62.3(4) | O(9A)–Tb(1)–O(4W) | 65.8(3) |

Symmetry code A: 1.5-*x*, -0.5+*y*, 0.5-*z*.

**Figure S1.** The chemical structure of 2,2',3,3'-oxydiphthalic acid ($H_4ODA$).

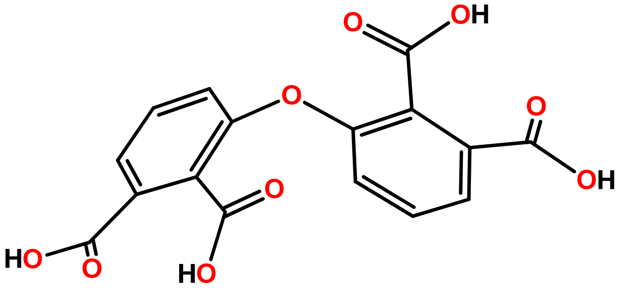

**Figure S2.** (a) The fluorescence spectra of Tb−HODA (0.33 g/L) in water solution upon the addition of 0.24 mM of Fe$^{3+}$. (b) The Stern−Volmer plot of Tb−HODA quenched by Fe$^{3+}$ aqueous solution.

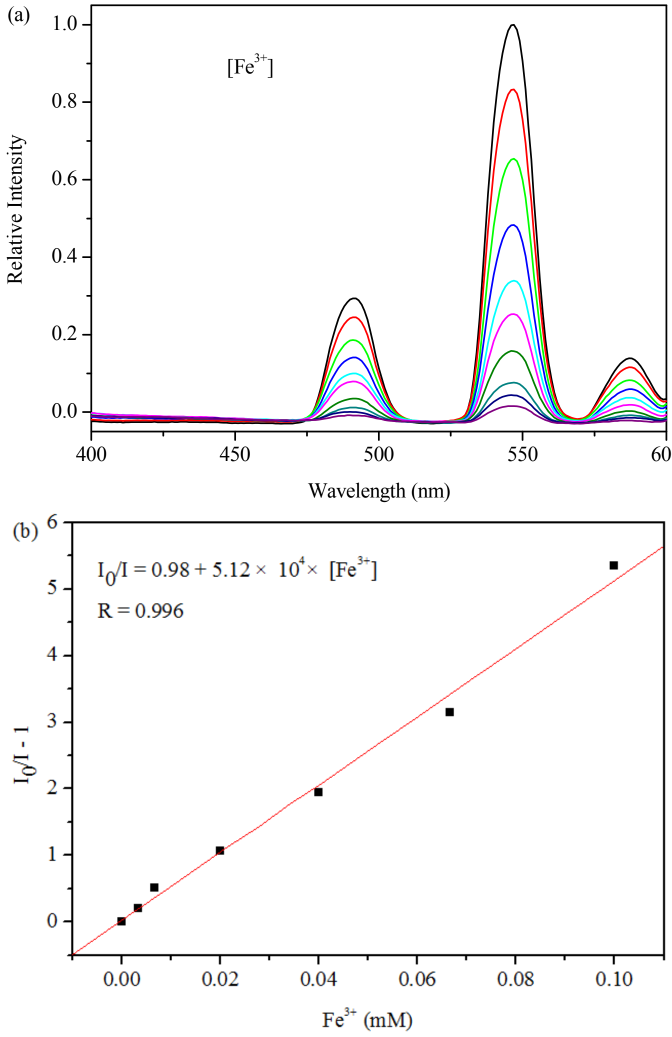

**Figure S3.** The fluorescence spectra of Tb−HODA (0.33 g/L) in water solution upon the addition of 0.48 mM of various metal ions, respectively.

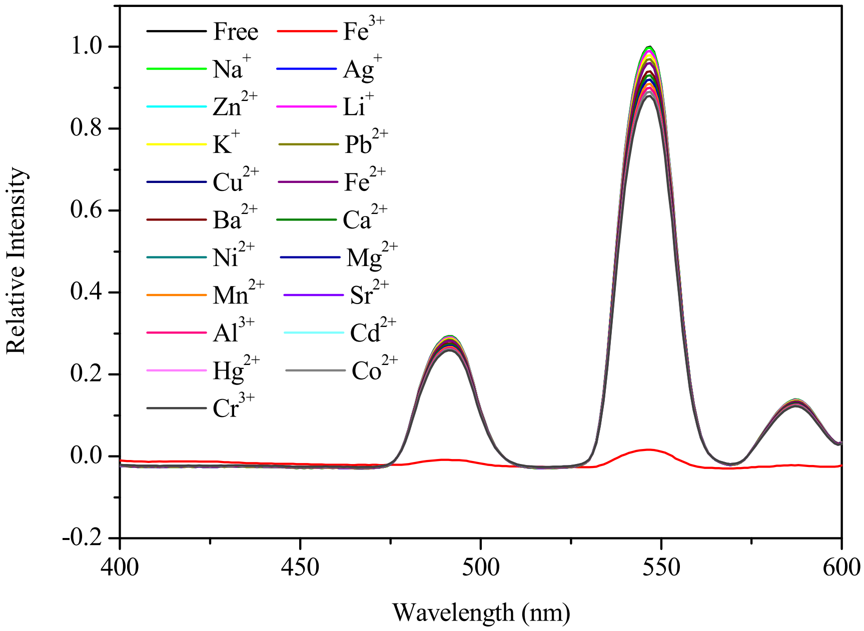

**Figure S4.** The fluorescence response of compound Tb−HODA (0.33 g/L) in water at different pH values.

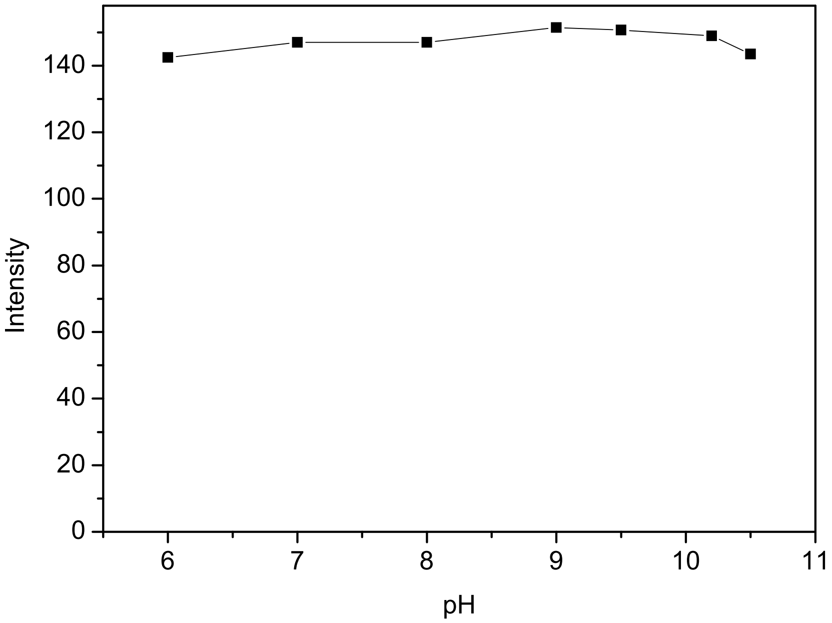

**Figure S5.** Fluorescence spectrum of Tb−HODA (0.33 g/L) in water (black line) and with 0.04 mM $Fe^{3+}$ (red line) followed by the treatment with glutathione (10 equiv of $Fe^{3+}$, green line) or EDTA/base (10 equiv of $Fe^{3+}$, blue line).

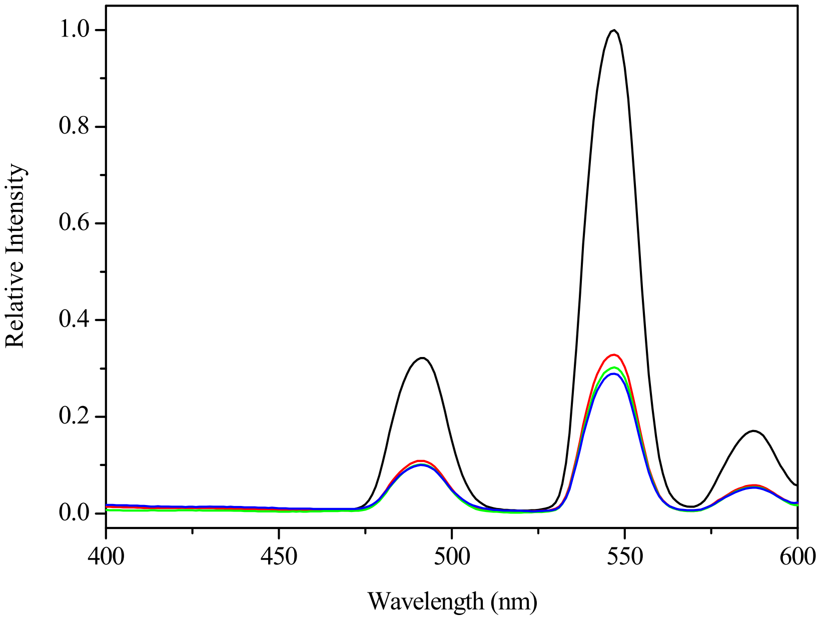

**Figure S6.** Powder X−ray diffraction (XRD) profiles for as-synthesized Tb−HODA (black), Tb−HODA treated in $Fe^{3+}$ solution for one day (red) and Tb−HODA⊐$Fe^{3+}$ samples after the third cycles (green).

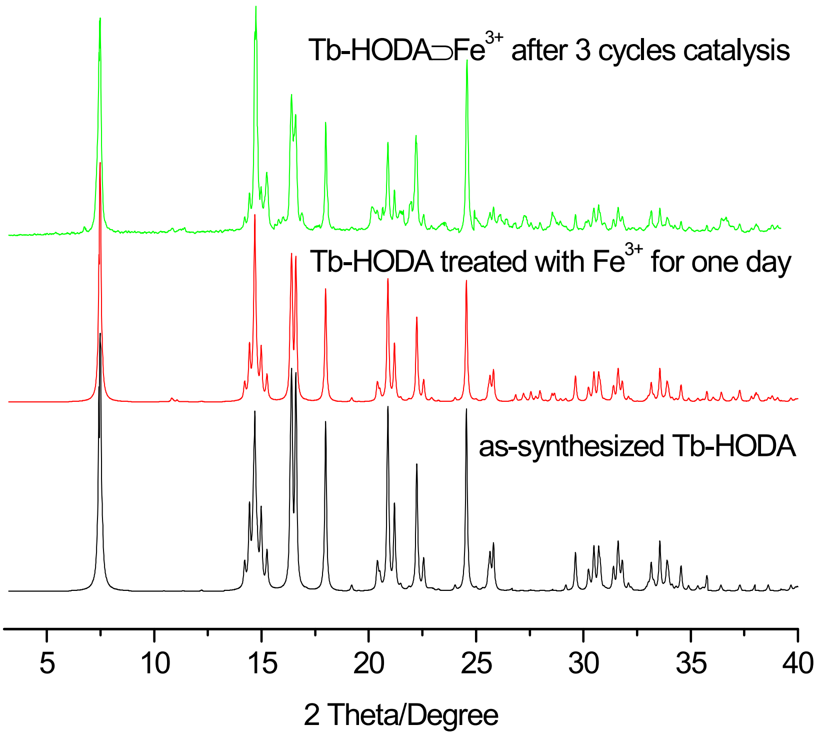

**Table S2** Comparison of the detective sensitivity in various MOFs for $Fe^{3+}$.

| No. | MOF | Detection limit | Ref. |
|---|---|---|---|
| 1 | FJU-13a-Eu<br>FJU-13a-Tb | 1.41 μM<br>1.01 μM | S1 |
| 2 | $[Eu(bpda)_{1.5}]H_2O\}_n$ | 0.9 μM | S2 |
| 3 | BUT-14 | 3.8 μM | S3 |
| 4 | BUT-15<br>$\{[Eu_2K_2(dcppa)_2(H_2O)_6]\cdot 5H_2O\}_n$ | 0.8 μM<br>1.0 μM | S4 |
| 5 | $Eu^{3+}$@MIL-53-COOH (Al) | 0.5 μM | S5 |
| 6 | $Eu_4L_3$ | 10 μM | S6 |
| 7 | $\{[Cd_3(HL)_2(H_2O)_3]\cdot 3H_2O\cdot 2CH_3CN\}_n$ | 90.6 μM | S7 |
| 8 | PCN-604 | 6.2 μM | S8 |
| 9 | Tb−MOF | 1.0 μM | S9 |
| 10 | 534-MOF-Tb | 0.13 mM | S10 |
| 11 | $[Cd(\mu_6\text{-cpta})_2(py)_2]_n$ | 0.21 mM | S11 |
| 12 | Tb-HIAAC | 70 nM | S12 |
| 13 | **Tb−HODA** | **20 nM** | **This work** |

**Table S3** Comparison of the performance of Tb−HODA⊃$Fe^{3+}$ with other catalysts for the conversion of glucose to HMF.

| No. | Catalyst | Glucose Con. [a] | Temp. (°C) | Time (hr) | Yield (%) | Ref. |
|---|---|---|---|---|---|---|
| 1 | $TiO_2/Nb_2O_5\cdot nH_2O$ (0.68) | 5.0% | 150 | 300 | 42 | S13 |
| 2 | Sn-Beta/HCl | 10.0% | 140 | 120 | 7.9 | S14 |
| 3 | $SO_4/ZrO_2$ | 0.5% | 100 | 360 | 10.0 | S15 |
| 4 | Beta-Cal750 | 2.4% | 180 | 60 | 20.2 | S16 |
| 5 | $TaOPO_4$ | 3.0% | 170 | 60 | 18.5 | S17 |
| 6 | MIL-101(Cr)-$SO_3H$ | 2.9% | 150 | 3 | 44 | S18 |
| 7 | MIL-$SO_3H$ | 4.9% | 130 | 24 | 29 | S19 |
| 8 | $PO_4$/NU(half) | 1.77% | 140 | 5 | 15 | S20 |
|  |  | 0.02% | 140 | 5 | 64 |  |
| 9 | UiO-66 | 4.35% | 160 | 0.5 | 28 | S21 |
|  |  | 4.36% | 160 | 0.5 | 37 |  |
| 10 | **Tb−HODA⊃$Fe^{3+}$** | **2.1%** | **140** | **2.5** | **48.7** | **This work** |

[a] Glucose con. = $m_{glucose}/(m_{glucose} + m_{solvent})$, $m_{glucose}$ is the quality of glucose and $m_{solvent}$ is the quality of solvent.

**Reference:**

S1. L. Liu, Y. Wang, R. Lin, Z. Yao, Q. Lin, L. Wang, Z. Zhang and S. Xiang, *Dalton Trans.*, 2018, **47**, 16190-16196.

S2. J. Wang, J. Wang, Y. Li, M. Jiang, L. Zhang and P. Wu, *New J. Chem.*, 2016, **40**, 8600-8606.

S3. B. Wang, Q. Yang, C. Guo, Y. Sun, L.-H. Xie and J.-R. Li, *ACS Appl. Mater. Interfaces*, 2017, **9**, 10286-10295.

S4. H. Zhang, R. Fan, W. Chen, J. Fan, Y. Dong, Y. Song, X. Du, P. Wang and Y. Yang, *Cryst. Growth Des.*, 2016, **16**, 5429-5440.

S5. Y. Zhou, H.-H. Chen and B. Yan, *J. Mater. Chem. A*, 2014, **2**, 13691-13697.

S6. W. Liu, X. Huang, C. Xu, C. Chen, L. Yang, W. Dou, W. Chen, H. Yang and W. Liu, *Chem. Eur. J.*, 2016, **22**, 18769-18776.

S7. W.-Q. Tong, W.-N. Liu, J.-G. Cheng, P.-F. Zhang, G.-P. Li, L. Hou and Y.-Y. Wang, *Dalton Trans.*, 2018, **47**, 9466-9473.

S8. Y. Zhang, X. Yang and H.-C. Zhou, *Dalton Trans.*, 2018, **47**, 11806-11811.

S9. Q. Zhang, J. Wang, A. M. Kirillov, W. Dou, C. Xu, C. Xu, L. Yang, R. Fang and W. Liu, *ACS Appl. Mater. Interfaces*, 2018, **10**, 23976-23986.

S10. M. Chen, W.-M. Xu, J.-Y. Tian, H. Cui, J.-X. Zhang, C.-S. Liu and M. Du, *J. Mater. Chem. C*, 2017, **5**, 2015-2021.

S11. J.-Z. Gu, X.-X. Liang, Y.-H. Cui, J. Wu, Z.-F. Shi and A. M. Kirillov, *CrystEngComm*, 2017, **19**, 2570-2588.

S12. M. Huangfu, X. Tian, S. Zhao, P. Wu, H. Chu, X. Zheng, J. Tang and J. Wang, *New J. Chem.*, 2019, **43**, 10232-10236.

S13. F. Huang, T. Jiang, X. Xu, L. Chen, G. Laurenczy, Z. Fei and P. J. Dyson, *Catal. Sci. Technol.*, 2020, **10**, 7857-7864.

S14. P. Sudarsanam, E. Peeters, E. V. Makshina, V. I. Parvulescu and B. F. Sels, *Chem. Soc. Rev.*, 2019, **48**, 2366-2421.

S15. A. Osatiashtiani, A. F. Lee, D. R. Brown, J. A. Melero, G. Morales and K. Wilson, *Catal. Sci. Technol.*, 2014, **4**, 333-342.

S16. R. Otomo, T. Yokoi, J. N. Kondo and T. Tatsumi, *Appl. Catal. A: General.*, 2014, **470**, 318-326.

S17. I. Jiménez-Morales, A. Teckchandani-Ortiz, J. Santamaría-González, P. Maireles-Torres and A. Jiménez-López, *Appl. Catal. B-Environ.*, 2014, **144**, 22-28.

S18. Y. Su, G. Chang, Z. Zhang, H. Xing, B. Su, Q. Yang, Q. Ren, Y. Yang and Z. Bao, *AIChE J.*, 2016, **62**, 4403-4417.

S19. A. Herbst and C. Janiak, *New J. Chem.*, 2016, **40**, 7958-7967.

S20. M. Yabushita, P. Li, T. Islamoglu, H. Kobayashi, A. Fukuoka, O. K. Farha and A. Katz, *Ind. Eng. Chem. Res.*, 2017, **56**, 7141-7148.

S21. J. Gong, M. J. Katz and F. M. Kerton, *RSC Adv.*, 2018, **8**, 31618-31627.